

Research Article

Vibration Suppression Control of a Flexible Gantry Crane System with Varying Rope Length

Tung Lam Nguyen ¹, Trong Hieu Do,¹ and Hong Quang Nguyen ²

¹Hanoi University of Science and Technology, Vietnam

²Thai Nguyen University of Technology, Vietnam

Correspondence should be addressed to Tung Lam Nguyen; lam.nguyentung@hust.edu.vn

Received 4 October 2018; Revised 3 December 2018; Accepted 12 December 2018; Published 11 February 2019

Guest Editor: Quang Hieu Ngo

Copyright © 2019 Tung Lam Nguyen et al. This is an open access article distributed under the Creative Commons Attribution License, which permits unrestricted use, distribution, and reproduction in any medium, provided the original work is properly cited.

The paper presents a control approach to a flexible gantry crane system. From Hamilton's extended principle the equations of motion that characterized coupled transverse motions with varying rope length of the gantry is obtained. The equations of motion consist of a system of ordinary and partial differential equations. Lyapunov's direct method is used to derive the control located at the trolley end that can precisely position the gantry payload and minimize vibrations. The designed control is verified through extensive numerical simulations.

1. Introduction

Gantry cranes are essential for load handling operation in various fields. Due to the flexibility in the gantry system structure, there exists a trade-off between the requirement of fast operations and minimizing payload vibration. Currently, solving the aforementioned constraint is an open and promising research area.

Renowned for its simplicity in practical applications, input command shaping is one of the earliest attempts to crane control [1–6]. Maghsoudi et al. combine input shaping with particle swarm based optimization for a 3D gantry crane control problem in [7]. The improved method shows better performances in terms of vibration reduction with the presence of system friction and varying rope length. However, due to its open-loop structure, input shaping faces a serious difficulty in handling system with disturbances. Fulfilling this gap, Park et al. propose a feedback linearization for trolley and hoisting operations to guarantee asymptotic stability. Similarly, a partial feedback control is developed in [8]; the control is a linear combination of feedback linearization from actuated and unactuated dynamics. Subsequently, the closed-loop system is proven to be asymptotically stable. A novel motion-planning is designed based on minimum

time control principle in combination with swing suppression control which is formulated in [9] for a class of high speed hoisting cranes; a remarkable contribution of the paper is robustness and uncertainty independent of the kinematic model. An analogous idea of using predefined trajectories is adopted in [10] where the author achieves the optimal trajectory for the gantry by employing radial basic function networks assisted by a particle swarm optimization scheme. In the quest of avoiding dependence on system parameters and system robustness, Tuan et al. use sliding mode as a control core in conjunction with other techniques such as model reference adaptive control [11] for crane systems. In addition, variations of sliding mode control can be found in [12] where super twisting based sliding mode controls are considered. Different from traditional gantry system structure with control attached to the trolley end, Schlott et al. [13] propose an actuated load structure for decoupling control purpose. A visual feedback scheme is developed by Lee et al. [14], visual information of a 3D crane is sent to an adaptive fuzzy sliding mode control, and as a result the close-loop system possesses robustness and model-free nature. Several approaches to the gantry system were also mentioned in [15–17].

The above-mentioned works treat crane motion as pendulum-like motion where the crane cable is considered as a rigid body. Hence, the crane equations of motion consist of ordinary differential equations. In practice, the crane cable is flexible; this property leads to a requirement of a set of partial differential equations describing the crane motion. Joshi et al. [18] propose a control law based on Lyapunov stability for a flexible gantry. Similarly, looking at the gantry with flexible cable, D'Andréa-Novel et al. [19] design a feedback control that can stabilize the system exponentially. Considering the gantry with hoisting operation, Moustafe et al. [20] derive a boundary control for the system with varying rope length. With efforts to force payload vibration in a predefined range He et al. [21] formulate a control scheme for flexible gantry with a support of actuated payload and Nguyen et al. [22] develop control forces acting at the trolley end of a two-dimensional gantry.

In the paper, a position control and vibration suppression of a 3D gantry crane with varying rope length are considered. The contribution of the research is the formulation of 3D flexible gantry with coupling mechanism in transverse-transverse and transverse-longitudinal directions and the control designed for stabilizing the system. The system equations of motion are derived via Hamilton's extended principle. Subsequently, control forces are constructed based on Lyapunov's stability. Extensive simulations are presented to demonstrate the effectiveness of the proposed control.

2. Problem Formulation

Before deriving the gantry system mathematical model, the following is assumed:

- (1) Cable axial deformation is very small in comparison with the cable length.
- (2) The payload is considered as a point-mass.
- (3) Friction in trolley motion is ignored.
- (4) Environmental disturbances are neglected.
- (5) Moving mass in X and Y directions are equal.
- (6) The deflection angle of the cable from vertical axis is very small.
- (7) Diameter to length ratio of the cable is very large.

Assumption (1) implies that the axial deformation of the cable is ignored; however, transverse deformation is considered. Assumptions (2), (3), and (4) imply that the paper targets on small-size automated crane systems, where point-mass payload and zero disturbances assumptions are justified. Assumption (5) is placed to simplify the mathematical formulation process without loss of generality. Assumption (6) is generally accepted in practice. Assumption (7) suggests that string model is used.

The crane system coordinate is depicted in Figure 1, where $x(t)$ and $y(t)$ are the trolley positions in X and Y, respectively. A material point in Z direction is represented by $z(t)$ and $l(t)$ denotes the cable total length. The distance from a cable

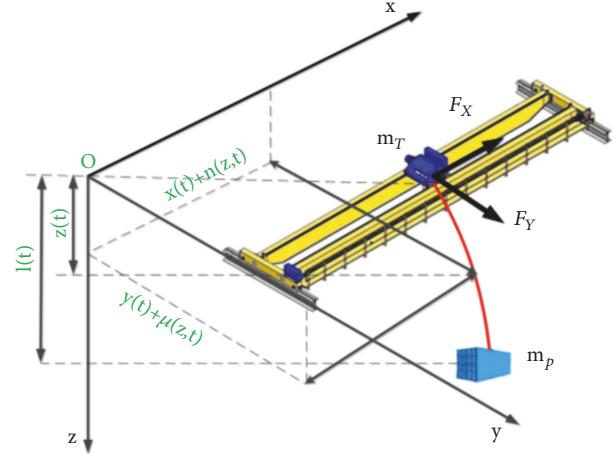


FIGURE 1: System coordinate.

material point to the trolley in X and Y directions is $n(t)$ and $\mu(t)$. The position vector of cable material point p is defined as

$$\vec{r}_p = [x(t) + n(z(t), t)] \vec{i} + [y(t) + \mu(z(t), t)] \vec{j} + z(t) \vec{k} \quad (1)$$

where \vec{i} and \vec{k} are unit vectors in X and Z directions, respectively. From (1), the velocity vector can be deduced as follows:

$$\begin{aligned} \vec{v}_p = & [x_t(t) + n_t(z(t), t) + z_t(t) n_z(z(t), t)] \vec{i} \\ & + [y_t(t) + \mu_t(z(t), t) + z_t(t) \mu_z(z(t), t)] \vec{j} \\ & + z_t(t) \vec{k} \end{aligned} \quad (2)$$

In similar fashion, the velocity vectors of the trolley and payload can be written as

$$\begin{aligned} \vec{v}_{m_p} = & [x_t(t) + \bar{n}_t(z(t), t) + l_t(t) \bar{n}_z(z(t), t)] \vec{i} \\ & + [y_t(t) + \bar{\mu}_t(z(t), t) + l_t(t) \bar{\mu}_z(z(t), t)] \vec{j} \\ & + l_t(t) \vec{k} \end{aligned} \quad (3)$$

and

$$\vec{v}_{m_T} = x_t(t) \vec{i} + y_t(t) \vec{j} \quad (4)$$

where $\bar{n}_t = \partial n(l(t), t) / \partial t$, $\bar{n}_z = \partial n(l(t), t) / \partial z$, $\bar{\mu}_t = \partial \mu(l(t), t) / \partial t$, $\bar{\mu}_z = \partial \mu(l(t), t) / \partial z$.

For the sake of clarity, from this point onward $(\bullet)_t$, $(\bullet)_{tt}$, $(\bullet)_z$, and $(\bullet)_{zz}$ are used to denote $\partial \bullet / \partial t$, $\partial^2 \bullet / \partial t^2$, $\partial \bullet / \partial z$, and $\partial^2 \bullet / \partial z^2$, respectively, and the argument (t) is dropped where there is no confusion. The system coordinate depicted

in Figure 1 suggests that the geometry boundary conditions for the crane system are

$$n(0, t) = n_t(0, t) = \mu(0, t) = \mu_t(0, t) = 0 \quad (5)$$

The total kinetic energy of the system induced by the cable, trolley, and payload motion is given by

$$\begin{aligned} KE = & \frac{1}{2} \rho \int_0^{l(t)} \left((x_t + n_t + z_t n_z)^2 + (y_t + \mu_t + z_t \mu_z)^2 \right. \\ & \left. + z_t^2 \right) dz + \frac{1}{2} m_T (x_t^2 + y_t^2) + \frac{1}{2} m_p \left((x_t + \bar{n}_t \right. \\ & \left. + l_t \bar{n}_z)^2 + (y_t + \bar{\mu}_t + l_t \bar{\mu}_z)^2 + l_t^2 \right) \end{aligned} \quad (6)$$

where ρ is the cable material density, m_T is the trolley mass, and m_p denotes the payload mass. The system potential energy is

$$\begin{aligned} PE = & \frac{1}{2} \int_0^{l(t)} (m_p g + \rho g (l - z)) (n_z^2 + \mu_z^2) dz \\ & + \frac{1}{2} EA \int_0^{l(t)} \left(\frac{1}{2} (n_z^2 + \mu_z^2) \right)^2 dz - m_p g l \\ & - \int_0^{l(t)} \rho g z dz \end{aligned} \quad (7)$$

where E is Young's modulus and A is the cable cross section area. The first term represents potential energy caused by the rope tension, the second term is the strain energy, and the two last terms are generated by gravity of the cable and payload. The virtual work is

$$W = F_X x + F_Y y + F_L l \quad (8)$$

The virtual work in (8) is generated by force acting on the trolley and winch in X , Y , and Z directions. Applying the extended Hamilton principle

$$\int_{t_1}^{t_2} (\delta KE - \delta PE + \delta W) dt = 0 \quad (9)$$

where δ is variation operation. Substituting (6), (7), and (8) into (9) and carefully integrating by parts results in the following equations of motion of the cable in X and Y directions

$$\begin{aligned} & \rho (x_{tt} + n_{tt} + z_{tt} n_z + z_t (2n_{zt} + z_t n_{zz})) \\ & = (T n_z)_z + \frac{1}{2} EA (3n_z^2 n_{zz} + n_{zz} \mu_z^2 + 2n_z \mu_z \mu_{zz}) \end{aligned} \quad (10)$$

$$\begin{aligned} & \rho (y_{tt} + \mu_{tt} + z_{tt} \mu_z + z_t (2\mu_{zt} + z_t \mu_{zz})) \\ & = (T \mu_z)_z + \frac{1}{2} EA (3\mu_z^2 \mu_{zz} + \mu_{zz} n_z^2 + 2\mu_z n_z n_{zz}) \end{aligned} \quad (11)$$

where $T = m_p g + \rho g (l - z)$. Governing equations of trolley motions in X and Y directions are given by

$$\begin{aligned} & \int_0^{l(t)} \rho (x_{tt} + n_{tt} + z_{tt} n_z + z_t (2n_{zt} + z_t n_{zz})) dz \\ & + m_T x_{tt} \\ & + m_p (x_{tt} + \bar{n}_{tt} + l_{tt} \bar{n}_z + l_t (2\bar{n}_{zt} + l_t \bar{n}_{zz})) = F_X \end{aligned} \quad (12)$$

$$\begin{aligned} & \int_0^{l(t)} \rho (y_{tt} + \mu_{tt} + z_{tt} \mu_z + z_t (2\mu_{zt} + z_t \mu_{zz})) dz \\ & + m_T y_{tt} \\ & + m_p (y_{tt} + \bar{\mu}_{tt} + l_{tt} \bar{\mu}_z + l_t (2\bar{\mu}_{zt} + l_t \bar{\mu}_{zz})) = F_Y \end{aligned} \quad (13)$$

Lowering and hoisting motions of the payload are represented by

$$\begin{aligned} & \int_0^{l(t)} \left\{ \rho [(x_{tt} + n_{tt} + z_{tt} n_z + z_t (2n_{zt} + z_t n_{zz})) n_z \right. \\ & + (\mu_{zt} + z_t \mu_{zz}) (y_t + \mu_t + z_t \mu_z) + z_{tt}] + T (n_z n_{zz} \\ & + \mu_z \mu_{zz}) + \frac{1}{2} (n_z^2 + \mu_z^2) (n_z n_{zz} + \mu_z \mu_{zz}) \left. \right\} dz \\ & + m_p [(x_{tt} + \bar{n}_{tt} + l_{tt} \bar{n}_z + l_t (2\bar{n}_{zt} + l_t \bar{n}_{zz})) \bar{n}_z + (y_{tt} \\ & + \bar{\mu}_{tt} + l_{tt} \bar{\mu}_z + l_t (2\bar{\mu}_{zt} + l_t \bar{\mu}_{zz})) \bar{\mu}_z + l_{tt}] - \frac{1}{2} \rho [(x_t \\ & + \bar{n}_t + l_t \bar{n}_z)^2 + (y_t + \bar{\mu}_t + l_t \bar{\mu}_z)^2 + l_t^2] + \frac{1}{2} m_p g (\bar{n}_z^2 \\ & + \bar{\mu}_z^2) + \frac{1}{2} EA \left(\frac{1}{2} (\bar{n}_z^2 + \bar{\mu}_z^2) \right)^2 = \bar{F}_l \end{aligned} \quad (14)$$

where $\bar{F}_l = F_l + m_p g + 2\rho g l$. The natural boundary conditions are

$$\begin{aligned} & \rho (x_t + \bar{n}_t + l_t \bar{n}_z) l_t - m_p g \bar{n}_z - \frac{1}{2} EA (\bar{n}_z^2 + \bar{\mu}_z^2) \bar{n}_z \\ & = m_p (x_{tt} + \bar{n}_{tt} + l_{tt} \bar{n}_z + l_t (2\bar{n}_{zt} + l_t \bar{n}_{zz})) \end{aligned} \quad (15)$$

$$\begin{aligned} & \rho (y_t + \bar{\mu}_t + l_t \bar{\mu}_z) l_t - m_p g \bar{\mu}_z - \frac{1}{2} EA (\bar{n}_z^2 + \bar{\mu}_z^2) \bar{\mu}_z \\ & = m_p (y_{tt} + \bar{\mu}_{tt} + l_{tt} \bar{\mu}_z + l_t (2\bar{\mu}_{zt} + l_t \bar{\mu}_{zz})) \end{aligned} \quad (16)$$

and the geometry boundary conditions given in (5). The system of equations describes the gantry dynamics including the cable deformation in X and Y directions with varying length. It is noted that, due to motion the cable flexibility, coupling mechanisms between transverse-transverse and transverse-longitudinal motions appear in the system dynamics. The coupling phenomenon causes a challenge in stabilizing the system. In addition, moving boundary at $l(t)$ due to lowering and hoisting motions makes the control problem even worse. The 3D crane dynamic is considered in the paper different from models given in [20] where only one transverse direction is considered and in [22] where the rope length is unchanged. The main contribution of the paper is formulation and control design process of the 3D crane system with dynamical couplings.

3. Control Design

The control objective is to simultaneously drive the payload to desired position while keeping swing angle as small as possible. In order to archive the control objective, consider the following Lyapunov candidate function

$$\begin{aligned}
 V(t) = & \frac{1}{2} \int_0^{l(t)} \left\{ \rho \left[(x_t + n_t + z_t n_z)^2 \right. \right. \\
 & + (y_t + \mu_t + z_t \mu_z)^2 + z_t^2 \left. \right] + T (n_z^2 + \mu_z^2) + \frac{1}{4} EA (n_z^2 \\
 & + \mu_z^2)^2 \left. \right\} dz + \frac{1}{2} k_1 m_T (x_t^2 + y_t^2) + \frac{1}{2} m_p \left[(x_t \right. \\
 & + \bar{n}_t + l_t \bar{n}_z)^2 + (y_t + \bar{\mu}_t + l_t \bar{\mu}_z)^2 + l_t^2 \left. \right] + \frac{1}{2} k_2 (x \\
 & - x_d)^2 + \frac{1}{2} k_3 (y - y_d)^2 + \frac{1}{2} k_4 (l - l_d)^2.
 \end{aligned} \quad (17)$$

where $k_i, i = 1, 2, 3, 4$ are strictly position constant and $x_d, y_d,$ and l_d are the desired position coordinates. The Lyapunov candidate function is radially unbounded and positive definite. It is also noted that the Lyapunov candidate function comprises the system kinetic, potential energy, and the error between current, and targeted positions. Differentiating (17) along the solutions of the equations of motion results in

$$\begin{aligned}
 \dot{V}(t) = & \int_0^{l(t)} \left\{ \rho \left[(x_t + n_t + z_t n_z) \right. \right. \\
 & \cdot (x_{tt} + n_{tt} + z_{tt} n_z + z_t (2n_{zt} + z_t n_{zz})) \\
 & + (y_t + \mu_t + z_t \mu_z) \\
 & \cdot (y_{tt} + \mu_{tt} + z_{tt} \mu_z + z_t (2\mu_{zt} + z_t \mu_{zz})) + z_t z_{tt} \left. \right] \\
 & + T (n_z n_{zz} z_t + n_z n_{zt} + \mu_z \mu_{zz} z_t + \mu_z \mu_{zt}) + \frac{1}{2}
 \end{aligned}$$

$$\begin{aligned}
 & \cdot EA (n_z^2 + \mu_z^2) (n_z n_{zz} z_t + n_z n_{zt} + \mu_z \mu_{zz} z_t \\
 & + \mu_z \mu_{zt}) \left. \right\} dz + \frac{1}{2} \rho l_t \left[(x_t + \bar{n}_t + l_t \bar{n}_z)^2 + (y_t \right. \\
 & + \bar{\mu}_t + l_t \bar{\mu}_z)^2 + l_t^2 \left. \right] + \frac{1}{2} m_p g l_t (\bar{n}_z^2 + \bar{\mu}_z^2) + \frac{1}{8} \\
 & \cdot EAl_t (\bar{n}_z^2 + \bar{\mu}_z^2)^2 + k_1 m_T (x_t x_{tt} + y_t y_{tt}) + m_p \left[(x_t \right. \\
 & + \bar{n}_t + l_t \bar{n}_z) (\beta x_{tt} + \bar{n}_{tt} + l_{tt} \bar{n}_z + l_t (2\bar{n}_{zt} + l_t \bar{n}_{zz})) \\
 & + (y_t + \bar{\mu}_t + l_t \bar{\mu}_z) (y_{tt} + \bar{\mu}_{tt} + l_{tt} \bar{\mu}_z + l_t (2\bar{\mu}_{zt} \\
 & + l_t \bar{\mu}_{zz})) + l_t l_{tt} \left. \right] + k_2 (x - x_d) x_t + k_3 (y - y_d) y_t \\
 & + k_4 (l - l_d) l_t
 \end{aligned} \quad (18)$$

Applying the equations of motion and boundary conditions, it can be shown that

$$\begin{aligned}
 \dot{V}(t) = & k_1 F_x x_t + k_2 (x - x_d) x_t + k_1 F_y y_t + k_3 (y \\
 & - y_d) y_t + \bar{F} l_t + k_4 (l - l_d) l_t + \int_0^{l(t)} n_t \left[(T n_z)_z \right. \\
 & + \frac{1}{2} EA (3n_z^2 n_{zz} + n_{zz} \mu_z^2 + 2n_z \mu_z \mu_{zz}) \left. \right] dz \\
 & + \int_0^{l(t)} \mu_t \left[(T \mu_z)_z \right. \\
 & + \frac{1}{2} EA (3\mu_z^2 \mu_{zz} + \mu_{zz} n_z^2 + 2\mu_z n_z n_{zz}) \left. \right] dz \\
 & + \frac{1}{2} EA \int_0^{l(t)} (n_z^2 + \mu_z^2) (n_z n_{zt} + \mu_z \mu_{zt}) dz \\
 & + \int_0^{l(t)} T (n_z n_{zt} + \mu_z \mu_{zt}) dz + \rho \bar{n}_t (x_t + \bar{n}_t \\
 & + l_t \bar{n}_z) l_t - m_p g \bar{n}_t \bar{n}_z - \frac{1}{2} EA \bar{n}_t (\bar{n}_z^2 + \bar{\mu}_z^2) \bar{n}_z \\
 & + \rho \bar{\mu}_t (y_t + \bar{\mu}_t + l_t \bar{\mu}_z) l_t - m_p g \bar{\mu}_t \bar{\mu}_z - \frac{1}{2} EA \bar{\mu}_t (\bar{n}_z^2 \\
 & + \bar{\mu}_z^2) \bar{\mu}_z + \rho l_t \left[(x_t + \bar{n}_t + l_t \bar{n}_z)^2 + (y_t + \bar{\mu}_t + l_t \bar{\mu}_z)^2 \right. \\
 & + l_t^2 \left. \right] + (1 - k_1) \int_0^{l(t)} x_t \left[(T n_z)_z \right. \\
 & + \frac{1}{2} EA (3n_z^2 n_{zz} + n_{zz} \mu_z^2 + 2n_z \mu_z \mu_{zz}) \left. \right] dz \\
 & + (1 - k_1) \int_0^{l(t)} y_t \left[(T \mu_z)_z
 \end{aligned}$$

$$\begin{aligned}
& + \frac{1}{2}EA \left(3\mu_z^2 \mu_{zz} + \mu_{zz} n_z^2 + 2\mu_z n_z n_{zz} \right) dz \\
& + (1 - k_1) x_t \left[\rho (x_t + \bar{n}_t + l_t \bar{n}_z) l_t - m_p g \bar{n}_z - \frac{1}{2} \right. \\
& \cdot EA \left(\bar{n}_z^2 + \bar{\mu}_z^2 \right) \bar{n}_z \left. \right] + (1 - k_1) y_t \left[\rho (y_t + \bar{\mu}_t + l_t \bar{\mu}_z) \right. \\
& \cdot l_t - m_p g \bar{\mu}_z - \frac{1}{2} EA \left(\bar{n}_z^2 + \bar{\mu}_z^2 \right) \bar{\mu}_z \left. \right]; \tag{19}
\end{aligned}$$

Carefully performing integration by parts leads to the following equation:

$$\begin{aligned}
\dot{V}(t) = & \left[\bar{F}_l + k_4 (l - l_d) \right. \\
& \left. + \rho \left((x_t + \bar{n}_t + l_t \bar{n}_z)^2 + (y_t + \bar{\mu}_t + l_t \bar{\mu}_z)^2 + l_t^2 \right) \right]
\end{aligned}$$

$$\begin{aligned}
& + \rho (x_t + \bar{n}_t + l_t \bar{n}_z) (\bar{n}_t + (1 - k_1) x_t) \\
& + \rho (y_t + \bar{\mu}_t + l_t \bar{\mu}_z) (\bar{\mu}_t + (1 - k_1) y_t) \left] l_t + \left[k_1 F_X \right. \right. \\
& + k_2 (x - x_d) - (1 - k_1) \\
& \cdot \left((Tn_z)_0 + \frac{1}{2} EA (n_z^3)_0 + \frac{1}{2} EA (n_z \mu_z^2)_0 \right) \left. \right] x_t \\
& + \left[k_1 F_X + k_3 (y - y_d) - (1 - k_1) \right. \\
& \cdot \left((T\mu_z)_0 + \frac{1}{2} EA (\mu_z^3)_0 + \frac{1}{2} EA (\mu_z n_z^2)_0 \right) \left. \right] y_t \tag{20}
\end{aligned}$$

The above equation suggests that control laws for three motions can be selected as

$$\begin{aligned}
\bar{F}_l = & -k_4 (l - l_d) - \rho \left((x_t + \bar{n}_t + l_t \bar{n}_z)^2 + (y_t + \bar{\mu}_t + l_t \bar{\mu}_z)^2 + l_t^2 \right) - \rho (x_t + \bar{n}_t + l_t \bar{n}_z) (\bar{n}_t + (1 - k_1) x_t) \\
& - \rho (y_t + \bar{\mu}_t + l_t \bar{\mu}_z) (\bar{\mu}_t + (1 - k_1) y_t) - k_1 l_t \tag{21}
\end{aligned}$$

$$F_X = \frac{\left[-k_2 (x - x_d) + (1 - k_1) \left((Tn_z)_0 + (1/2) EA (n_z^3)_0 + (1/2) EA (n_z \mu_z^2)_0 \right) - k_x x_t \right]}{k_1} \tag{22}$$

$$F_Y = \frac{\left[-k_3 (y - y_d) + (1 - k_1) \left((T\mu_z)_0 + (1/2) EA (\mu_z^3)_0 + (1/2) EA (\mu_z n_z^2)_0 \right) - k_y y_t \right]}{k_1} \tag{23}$$

where k_x , k_y , and k_l are strictly positive constant. It should be noted again that the derived controls are located at the trolley end. The selected controls render time derivative of the Lyapunov function candidate as

$$\dot{V}(t) = -k_l l_t^2 - k_x x_t^2 - k_y y_t^2 < 0 \tag{24}$$

The inequality suggests that the close loop system is stable in Lyapunov's sense.

4. Simulation Results

Numerical simulations for illustrating the ability of positioning trolley and suppressing payload swing angle of the proposed control are given in this section. Initially, the payload is located at (0,0,0); the system is designed to move the payload to the desired position at (15,20,5). The system simulation parameters are

$$m_T = 5kg;$$

$$m_p = 15kg;$$

$$EA = 0.3N;$$

$$\rho = 0.1kg/m$$

(25)

Firstly, the positioning problem is considered regardless of the payload vibration. It can be observed from Figures 2–7 that the desired position is reached; however, there exists payload vibration.

Secondly, the proposed control for positioning and vibration suppressing is activated. The simulation results in Figures 8–13 show that the effectiveness of the control is confirmed. Control forces are in a practical range. It can be observed that control forces in uncontrolled cases have a tendency of abrupt changing compared to controlled cases. The phenomenon is predicted since vibration of the payload directly affects the trolley motion and leads to changes in control forces.

In addition, because payload vibration is fed back to the trolley, control effort is lower in controlled cases.

5. Conclusions

In the paper, position and vibration suppression problems in the gantry crane system with flexible cable are considered.

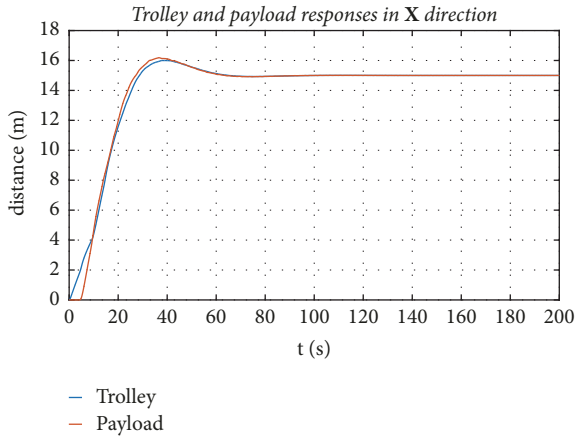


FIGURE 2: Trolley and payload responses in X direction without vibration control.

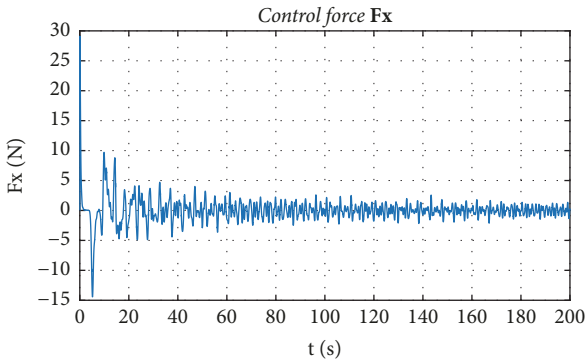


FIGURE 3: Control force F_x without vibration control.

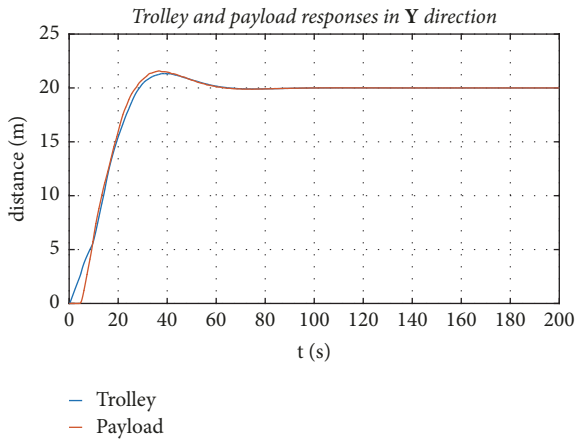


FIGURE 4: Trolley and payload responses in Y direction without vibration control.

Based on system energy analysis equations of motion that govern the gantry dynamics deforming in two transverse directions with varying cable length is derived according to Hamilton's extended principle. The process results in a system of ordinary and partial differential equations including cable dynamics and boundary conditions at trolley and payload ends. Control forces that solve the control problem are

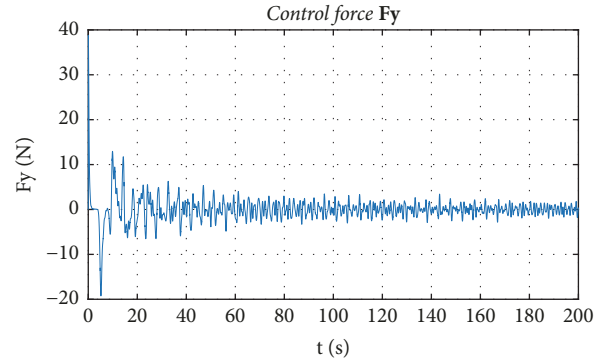


FIGURE 5: Control force F_y without vibration control.

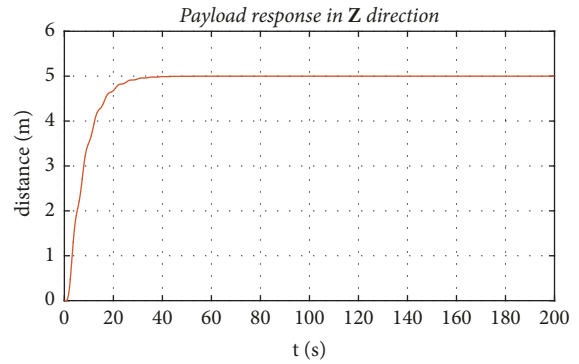


FIGURE 6: Payload response in Z direction without vibration control.

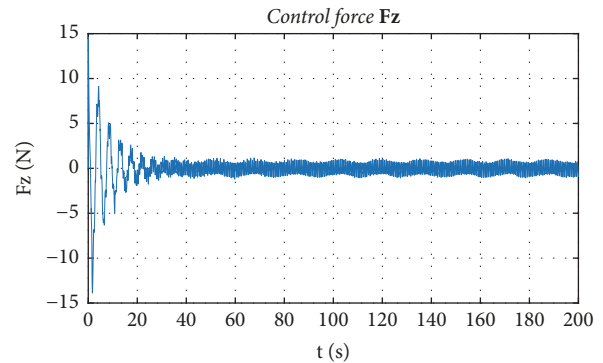


FIGURE 7: Control force F_z without vibration control.

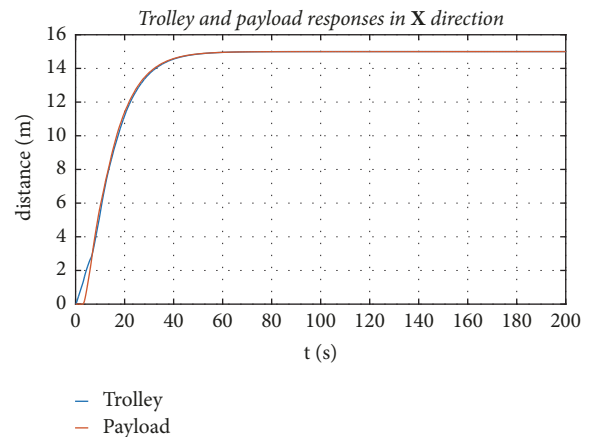
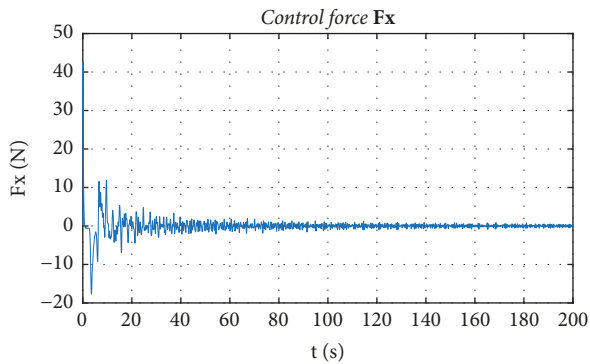
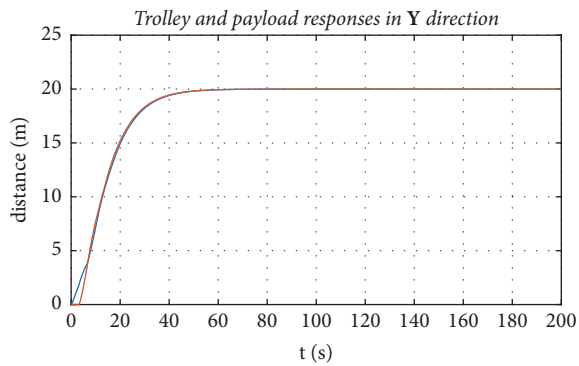
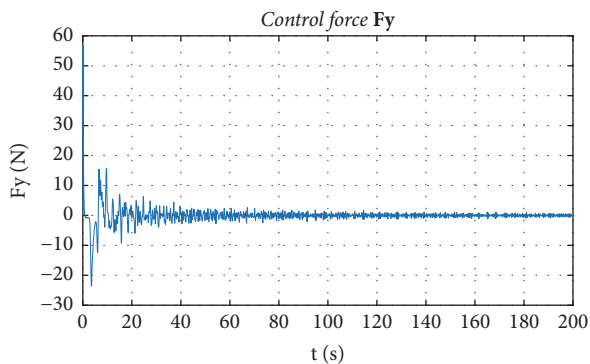


FIGURE 8: Trolley and payload responses in X direction with vibration control.

FIGURE 9: Control force F_x with vibration control.

— Trolley
— Payload

FIGURE 10: Trolley and payload responses in Y direction with vibration control.

FIGURE 11: Control force F_y with vibration control.

designed based on Lyapunov's direct method. The control forces are placed at trolley end of the gantry. Simulations are given to illustrate the effectiveness of the proposed control. System friction, input, and output constraints are the main target in the future research.

Data Availability

This publication is supported by multiple datasets, which are available at locations cited in the reference section.

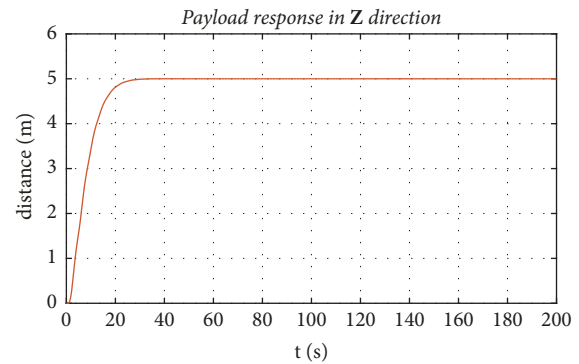
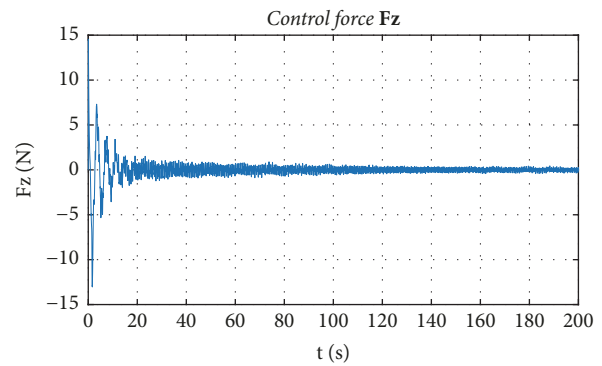


FIGURE 12: Payload response in Z direction with vibration control.

FIGURE 13: Control force F_z with vibration control.

Conflicts of Interest

The authors declare that they have no conflicts of interest.

References

- [1] W. Singhose, "Command shaping for flexible systems: a review of the first 50 years," *International Journal of Precision Engineering and Manufacturing*, vol. 10, no. 4, pp. 153–168, 2009.
- [2] J. Vaughan, E. Maleki, and W. Singhose, "Advantages of using command shaping over feedback for crane control," in *Proceedings of the 2010 American Control Conference, ACC 2010*, pp. 2308–2313, USA, July 2010.
- [3] J. Vaughan, A. Karajgikar, and W. Singhose, "A study of crane operator performance comparing PD-control and input shaping," in *Proceedings of the 2011 American Control Conference, ACC 2011*, pp. 545–550, USA, July 2011.
- [4] M. A. Ahmad, R. M. T. Raja Ismail, and M. S. Ramli, "Hybrid input shaping and non-collocated PID control of a gantry crane system: Comparative assessment," in *Proceedings of the 2009 IEEE/ASME International Conference on Advanced Intelligent Mechatronics, AIM 2009*, pp. 1792–1797, Singapore, July 2009.
- [5] M. A. Ahmad, Z. Zulkifely, and M. A. Zawawi, "Experimental investigations of input shaping schemes for sway control of a gantry crane system," in *Proceedings of the 2nd International Conference on Computer and Network Technology, ICCNT 2010*, no. 1, pp. 483–486, 2010.
- [6] A. Khalid, J. Huey, W. Singhose, J. Lawrence, and D. Frakes, "Human operator performance testing using an input-shaped

- bridge crane,” *Journal of Dynamic Systems, Measurement, and Control*, vol. 128, no. 4, pp. 835–841, 2006.
- [7] M. J. Maghsoudi, Z. Mohamed, S. Sudin, S. Buyamin, H. Jaafar, and S. Ahmad, “An improved input shaping design for an efficient sway control of a nonlinear 3D overhead crane with friction,” *Mechanical Systems and Signal Processing*, vol. 92, pp. 364–378, 2017.
 - [8] L. A. Tuan, G.-H. Kim, and S.-G. Lee, “Partial feedback linearization control of the three dimensional overhead crane,” in *IEEE International Conference on Automation Science and Engineering*, pp. 1198–1203, 2012.
 - [9] H.-H. Lee, “A new motion-planning scheme for overhead cranes with high-speed hoisting,” *Journal of Dynamic Systems, Measurement, and Control*, vol. 126, no. 2, pp. 359–364, 2004.
 - [10] A. Abe, “Anti-sway control for overhead cranes using neural networks,” *International Journal of Innovative Computing, Information and Control*, vol. 7, no. 7 B, pp. 4251–4262, 2011.
 - [11] L. A. Tuan, S.-G. Lee, L. C. Nho, and H. M. Cuong, “Robust controls for ship-mounted container cranes with viscoelastic foundation and flexible hoisting cable,” *Proceedings of the Institution of Mechanical Engineers, Part I: Journal of Systems and Control Engineering*, vol. 229, no. 7, pp. 662–674, 2015.
 - [12] C. Vazquez, J. Collado, and L. Fridman, “Super twisting control of a parametrically excited overhead crane,” *Journal of The Franklin Institute*, vol. 351, no. 4, pp. 2283–2298, 2014.
 - [13] P. Schlott and O. Sawodny, “Decoupling control for a gantry crane with an actuated load,” in *Proceedings of the 2012 7th IEEE Conference on Industrial Electronics and Applications, ICIEA 2012*, pp. 1610–1615, Singapore, July 2012.
 - [14] L.-H. Lee, C.-H. Huang, S.-C. Ku, Z.-H. Yang, and C.-Y. Chang, “Efficient visual feedback method to control a three-dimensional overhead crane,” *IEEE Transactions on Industrial Electronics*, vol. 61, no. 8, pp. 4073–4083, 2014.
 - [15] R. Toxqui, Y. Wen, and L. Xiaou, “Anti-swing control for overhead crane with neural compensation,” in *Proceedings of the International Joint Conference on Neural Networks 2006, IJCNN '06*, pp. 4697–4703, Canada, July 2006.
 - [16] D. Antic, Z. Jovanovic, S. Peric, S. Nikolic, M. Milojkovic, and M. Milosevic, “Anti-swing fuzzy controller applied in a 3d crane system,” *Engineering, Technology & Applied Science Research (ETASR)*, vol. 2, pp. 196–200, 2012.
 - [17] S. W. Su, H. T. Nguyen, R. Jarman et al., “Model predictive control of gantry crane with input nonlinearity compensation,” in *International Conference on Control, Automation and Systems Engineering*, pp. 312–316, 2009.
 - [18] S. Joshi and C. D. Rahn, “Position control of a flexible cable gantry crane: theory and experiment,” in *Proceedings of the 1995 American Control Conference. Part 1 (of 6)*, pp. 2820–2824, June 1995.
 - [19] B. D’Andréa-Novel and J. M. Coron, “Exponential stabilization of an overhead crane with flexible cable via a back-stepping approach,” *Automatica*, vol. 36, no. 4, pp. 587–593, 2000.
 - [20] K. A. F. Moustafa, M. B. Trabia, and M. I. Ismail, “Stability analysis and control of overhead crane with time-dependent flexible cable,” *Control*, pp. 24–28, 2005.
 - [21] W. He, S. Zhang, and S. S. Ge, “Adaptive control of a flexible crane system with the boundary output constraint,” *IEEE Transactions on Industrial Electronics*, vol. 61, no. 8, pp. 4126–4133, 2014.
 - [22] T. L. Nguyen and M. D. Duong, “Nonlinear control of flexible two-dimensional overhead cranes,” in *Adaptive Robust Control Systems*, A. T. Le, Ed., chapter 16, Intechopen, 2018.

